

Project Number: MQP-REC-DYE1

The Synthesis and Spectral Properties of Conjugated Dye Systems

A Major Qualifying Project Report

Submitted to the Faculty of

WORCESTER POLYTECHNIC INSTITUTE

In partial fulfillment of the requirements for the

Degree of Bachelor of Science

By:

Jennifer R. Ewalt

March 10, 2009

Approved by:

Prof. Robert E. Connors, Ph.D.
Project Advisor

Abstract

Dyes are important in many different applications, such as photosensitizers, fluorescent solvent polarity probes, fluoroionophores, and nonlinear optical materials. In this MQP, the synthesis and spectral properties of a conjugated dye, namely 1, 9-bis-(p-dimethylamino)-nonane-1,3,6,8-tetraene-5-one, or 2dbmac, were explored. The electronic absorption and fluorescence properties were examined in various nonpolar and polar solvents. Solvatochromic shifts, particularly bathochromic, or red shifts, occurred in both its absorption and fluorescence spectra as a result of the solvent's polarity. In addition to the electronic absorption and fluorescence properties, the photophysical properties were also explored, particularly fluorescence quantum yield and fluorescence lifetime parameters. For example, the fluorescence lifetimes of 2dbmac ranged from 0.24 (2,2,2-trifluoroethanol) to 1.1ns (n-hexane). Upon calculating the fluorescence quantum yield and fluorescence lifetime parameters, first-order radiative and nonradiative rates of decay were calculated. Lastly, quantum chemical calculations, both DFT B3LYP 6-31G(d) geometry optimization and TD-DFT spectral calculations, were performed on the compound and the excited states were found to have a charge transfer and a (π , π^*) transition for S_1 state and an (n , π^*) transition for S_2 state.

Acknowledgements

I would like to thank Professor Robert E. Connors for the use of his laboratory and for all his help and guidance throughout this project. Also, I would like to thank Professor Destin Heilman for letting me borrow chemicals for last minute experimental procedures. Finally, I would like to thank Christopher Zoto for all his help, guidance and time he gave to assist me.

Table of Contents

Abstract.....	2
Acknowledgements.....	3
Table of Contents.....	4
List of Figures.....	5
List of Tables.....	6
Introduction.....	7
Experimental.....	11
Results and Discussion.....	17
Conclusions.....	34
References.....	35
Appendix A: Fluorescence Quantum Yield Sample Calculation.....	36
Appendix B: Fluorescence Lifetime Sample Calculation.....	41

List of Figures

Figure 1: General structure of 2,5-diarylidene cyclopentanones.....	7
Figure 2: 1,9-bis-(p-dimethylamino)-nonane-1,3,6,8-tetraene-5-one (2dbmac)	8
Figure 3: Jablonski diagram showing fluorescence with solvent relaxation ³	9
Figure 4: Reaction Mechanism for the synthesis of 2dbmac	11
Figure 5: (a) ¹ H and (b) ¹³ C NMR Spectra of 2dbmac in CDCl ₃ . ¹ H NMR: δ (ppm) = 7.54-7.48 (dd, 2H), 7.42-7.40 (d, 4H), 6.94-6.91 (d, 2H), 6.83-6.77 (dd, 2H), 6.71-6.69 (d, 4H), 6.51-6.47 (d, 2H), 3.03 (s, 12H). ¹³ C NMR δ (ppm) = 151.4, 144.2, 142.4, 129.2, 127.3, 124.8, 123.1, 112.4, 40.6.	13
Figure 6: Infrared Spectra of 2dbmac	14
Figure 7: Absorption and fluorescence spectra in (a) 2,2,2-trifluoroethanol; (b) 2-propanol; (c) ethyl acetate; (d) acetone; (e) benzene; (f) carbon disulfide.	19
Figure 8: Optical absorption and fluorescence spectra in polar protic solvents,.....	20
(a) 2,2,2-trifluoroethanol, (b) methanol, (c) ethanol, (d) 2-propanol, (e) 1-propanol, and (f) 1-butanol.	
Figure 9: Optical absorption and fluorescence spectra in polar aprotic solvents,	21
Figure 10: Optical absorption and fluorescence spectra in nonpolar solvents,	22
Figure 11: Plot of maximum absorption and fluorescent wave numbers of 2dbmac against Δf in various polar protic, polar aprotic and nonpolar solvents..	24
Figure 12: Plot of maximum absorption and fluorescent wave numbers of 2dbmac against E _T (30) in various polar protic, polar aprotic and nonpolar solvents.....	25
Figure 13: Plot of first-order decay constants as a function of fluorescent wavenumbers of 2dbmac in various aprotic and protic solvents.	26
Figure 14: Jablonski diagram of the effect of solvent on (π, π*) and (n, π*) states.	28
Figure 15: Plot of the fluorescence quantum yield of 2dbmac against ν _{fl} in various protic and aprotic solvents	29
Figure 16: Lippert-Mataga Plot of Stoke's shift (Δν) against Δf of 2dbmac in various polar protic, polar aprotic and nonpolar solvents.	31
Figure 17: Computed molecular orbitals of 2dbmac	32
Figure 18: Fluorescence Lifetime of 2dbmac in Acetonitrile.....	42

List of Tables

Table 1: Spectroscopic and photophysical characteristics of 2dbmac in various solvents.....	23
Table 2: Computed Molecular Orbital Calculations of 2dbmac	32
Table 3: Dipole and Atomic Charges for the trans/trans structure of 2dbmac	33
Table 4: Theoretical and Experimental Absorbance Maximums	33

Introduction

Conjugated compounds contain carbon-carbon double or triple bonds in a 1,3-relationship; the conjugated system is dependent on the partial overlap of the p atomic orbitals. Also, it is possible for two systems to be in cross-conjugation with each other instead of the linearly conjugated compounds, such as 1, 3-butadiene. For example, 1,9-bis-(p-dimethylamino)-nonane-1,3,6,8-tetraene-5-one (**2dbmac**), Figure 2, is just one example of the many cross-conjugated systems.

Past research of 2, 5-diarylidene cyclopentanones have received attention for plausible applications in a wide variety of areas. Connors and Ucak-Astarlioglu¹ previously reported the electronic structure and spectroscopic properties for a series of unsubstituted 2,5-diarylidene cyclopentanones in a variety of solvents, whose generic chemical structure is shown in Figure 1. Their research has involved investigating the electronic absorption and fluorescence properties of the all trans configurations of unsubstituted 2, 5-diarylidene cyclopentanones (R = H) with n = 1, 2, and 3.

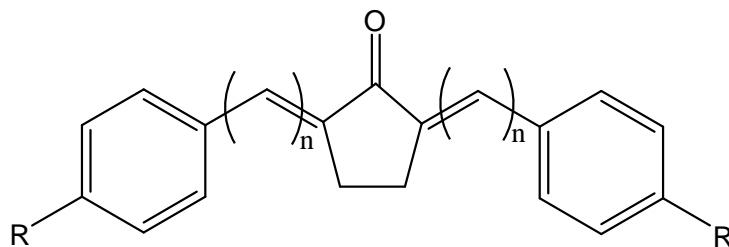


Figure 1: General structure of 2,5-diarylidene cyclopentanones

Research now includes studying a derivative with just the carbonyl compound at the cyclopentanone site, and electron donating groups covalently bonded at the para positions on the aromatic, specifically, alkylamino groups. The electronic structure and spectroscopy of 1,9-bis-(p-dimethylamino)-nonane-1,3,6,8-tetraene-5-one (**2dbmac**) has been studied in a variety of

nonpolar, polar protic and polar aprotic solvents, the chemical structure is shown in Figure 2. Investigation of the spectroscopic characteristics of **2dbmac** provides insight into the solvatochromic and photophysical properties of the compound in various solvent systems.

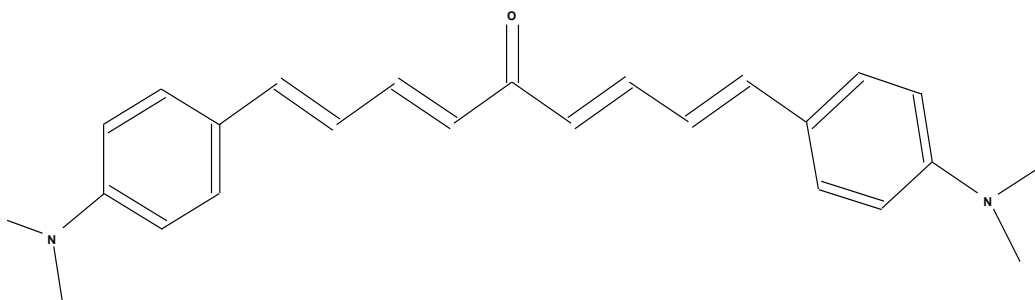


Figure 2: 1,9-bis-(p-dimethylamino)-nonane-1,3,6,8-tetraene-5-one (**2dbmac**)

Solvatochromism is the ability of a substance to physically change color with respect to solvent polarity². Depending on the nature of the solvent, solvatochromic molecules undergo either hypsochromic (blue) shifts or bathochromic (red) shifts in their optical absorption and fluorescence spectra. Theoretical and experimental observations confirm that solvatochromic molecules undergo bathochromic, or red shifts in going from nonpolar to polar aprotic and to polar protic solvents. A Jablonski state energy-level diagram, shown in Figure 3, illustrates the radiative processes of absorption and fluorescence with nonradiative solvent relaxation. When the ground state of a chemical species, with an electronic dipole moment of μ_g , is irradiated, the ground state species is promoted to the first-excited singlet state, with a dipole moment of μ_e . This process is then followed by nonradiative vibrational relaxation to the lowest energy vibrational state. The excited molecule relaxes on the order of 10^{-10} s (0.1 ns). The process of solvent relaxation involves forming a “solvent cage” appropriate for the charge distribution in an excited molecule, with the initial solvent cage appropriate for the charge distribution for the ground state in the molecule. The solvent’s reorientation results in a net stabilization of the

molecule-solvent system. This phenomenon is demonstrated by a red shift in the fluorescence relative to the absorption band, also known as (Stoke's shift). Stoke's shift for a molecule that has undergone a charge transfer transition upon excitation is greater in polar solvent than it is in nonpolar solvents, see Figure 3.

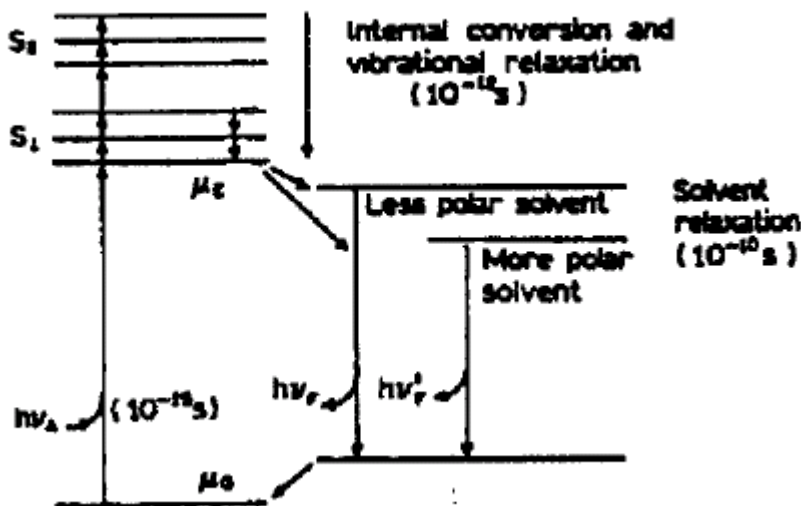


Figure 3: Jablonski diagram showing fluorescence with solvent relaxation³.

The primary focus in this paper is the synthesis, spectroscopic and photophysical characteristics of **2dbmac** in solvents of different polarity and hydrogen bonding capacity. Photophysical properties involve determining absorption and fluorescence spectra as well as fluorescence quantum yields (Φ_f) and fluorescence lifetimes (τ_f) in various nonpolar, polar aprotic and polar protic solvent systems. Both first-order radiative and nonradiative decay constants were calculated upon the knowledge of both Φ_f and τ_f .

Additionally, quantum chemical calculations were performed on the compound and two isomers (a cis/trans structure and a cis/cis structure). Computational calculations confirm that the structures have similar properties, particularly the ground state dipole moment and the atomic

charges of the tertiary nitrogen and the carbonyl oxygen. Calculations of the original trans/trans structure of 2dbmac show that the $S_0 \rightarrow S_1$ electronic transition occurs via an intramolecular charge transfer (π, π^*) mechanism and the $S_0 \rightarrow S_2$ transition is predicted to be (n, π^*) for the compound. The results suggest that **2dbmac** has potential as a solvent polarity probe since it meets some of the requirements, including charge transfer, solvatochromic shifts and a large difference between the excited and ground state dipoles.

Experimental

1. Synthesis of 2dbmac

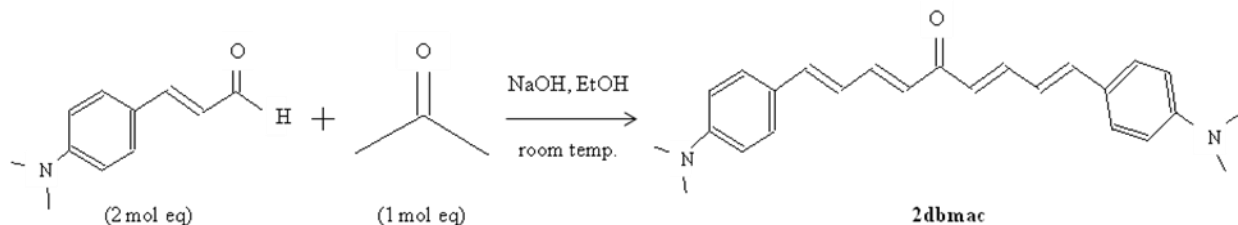
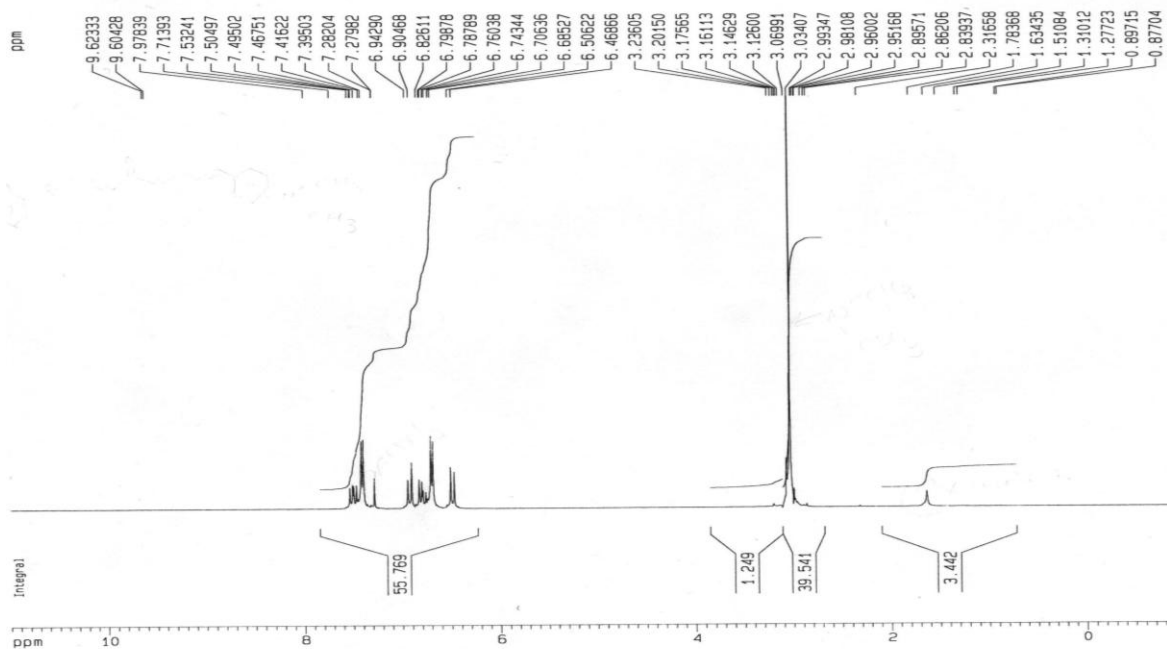


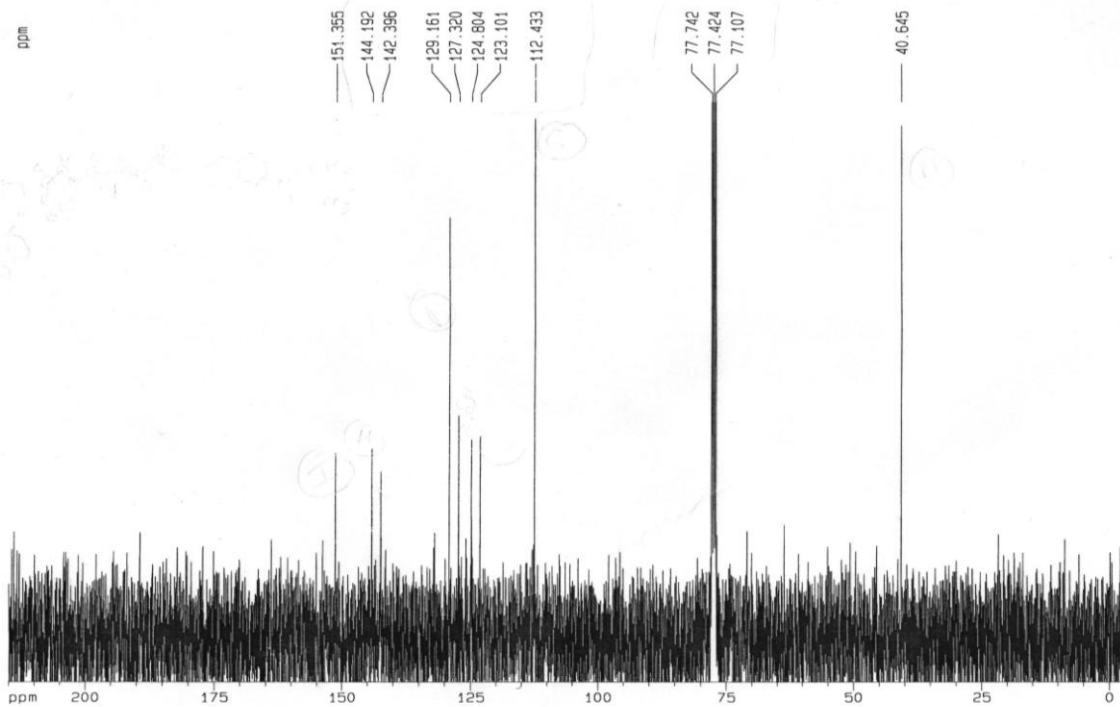
Figure 4: Reaction Mechanism for the synthesis of **2dbmac**

The synthesis of **2dbmac** involves an intermolecular base-catalyzed condensation reaction between spec. grade acetone (1 mol equivalent) and p- dimethylaminocinnamaldehyde (2 mol equivalents) at room temperature. The synthesis was followed by recrystallization with pure ethanol. The typical reaction mechanism for a crossed aldol condensation reaction is as follows. In a clean Erlenmeyer flask (50mL), containing a magnetic stir bar, acetone (0.005mol, 0.367mL) was added first, followed by a 20% Sodium Hydroxide (4mL) solution in deionized water, added drop by drop to the stirring solution. This solution was set aside for 30 minutes, with continuous stirring, to form the enolate intermediate. After enolate formation, p- dimethylaminocinnamaldehyde (0.01mol, 1.752g) was slowly added to the flask to initiate the reaction. Any remaining solid left on the weigh boat was washed with ethanol (15mL) and the resulting solution was added to the reaction flask. The reaction flask was corked, covered with foil to prevent light decomposition due to the photosensitivity of the compounds, and the reaction flask was left to react overnight. The resulting solution was tested by TLC to determine the extent of the reaction. Once the reaction was complete, the solid was collected by suction filtration and washed with deionized water (4 by 25mL) to remove all of the sodium hydroxide.

The solid was left on the vacuum to suction dry for a few hours and then pressed dried between two sheets of filter paper. The product was analyzed first by proton NMR, and the resulting NMR revealed impurities. The product was then recrystallized using pure ethanol and then analyzed again by proton and carbon 13 NMR and IR. Analysis of the NMR of the purified product showed no impurities left in the compound. The reaction mechanism for **2dbmac** is shown in Figure 4, the ^1H and ^{13}C NMR are depicted in Figures 5 (a) and (b), and the IR is shown in Figure 6.



(a)



(b)

Figure 5: (a) ^1H and (b) ^{13}C NMR Spectra of 2dbmac in CDCl_3 . ^1H NMR: δ (ppm) = 7.54-7.48 (dd, 2H), 7.42-7.40 (d, 4H), 6.94-6.91 (d, 2H), 6.83-6.77 (dd, 2H), 6.71-6.69 (d, 4H), 6.51-6.47 (d, 2H), 3.03 (s, 12H). ^{13}C NMR δ (ppm) = 151.4, 144.2, 142.4, 129.2, 127.3, 124.8, 123.1, 112.4, 40.6.

2. Spectrophotometric Analysis

For the spectrophotometric analysis, UV/Vis, fluorescence, NMR, and IR spectra needed to be collected and analyzed. All of the spectra were collected on different instrument and are as follows. The Ultraviolet/Visible spectra were measured using a Perkin Elmer[®] Lambda 35 UV/VIS spectrometer with 2nm band-passes. The fluorescence spectra were obtained using a Perkin Elmer[®] LS 50B luminescence spectrophotometer that is equipped with a R928 phototube detector. The NMR spectra were obtained using a Bruker[®] AVANCE 400MHz spectrometer. Lastly, the IR spectra were obtained using a Perkin Elmer[®] Spectrum One FT-IR spectrometer. The IR spectrum is shown in Figure 6.

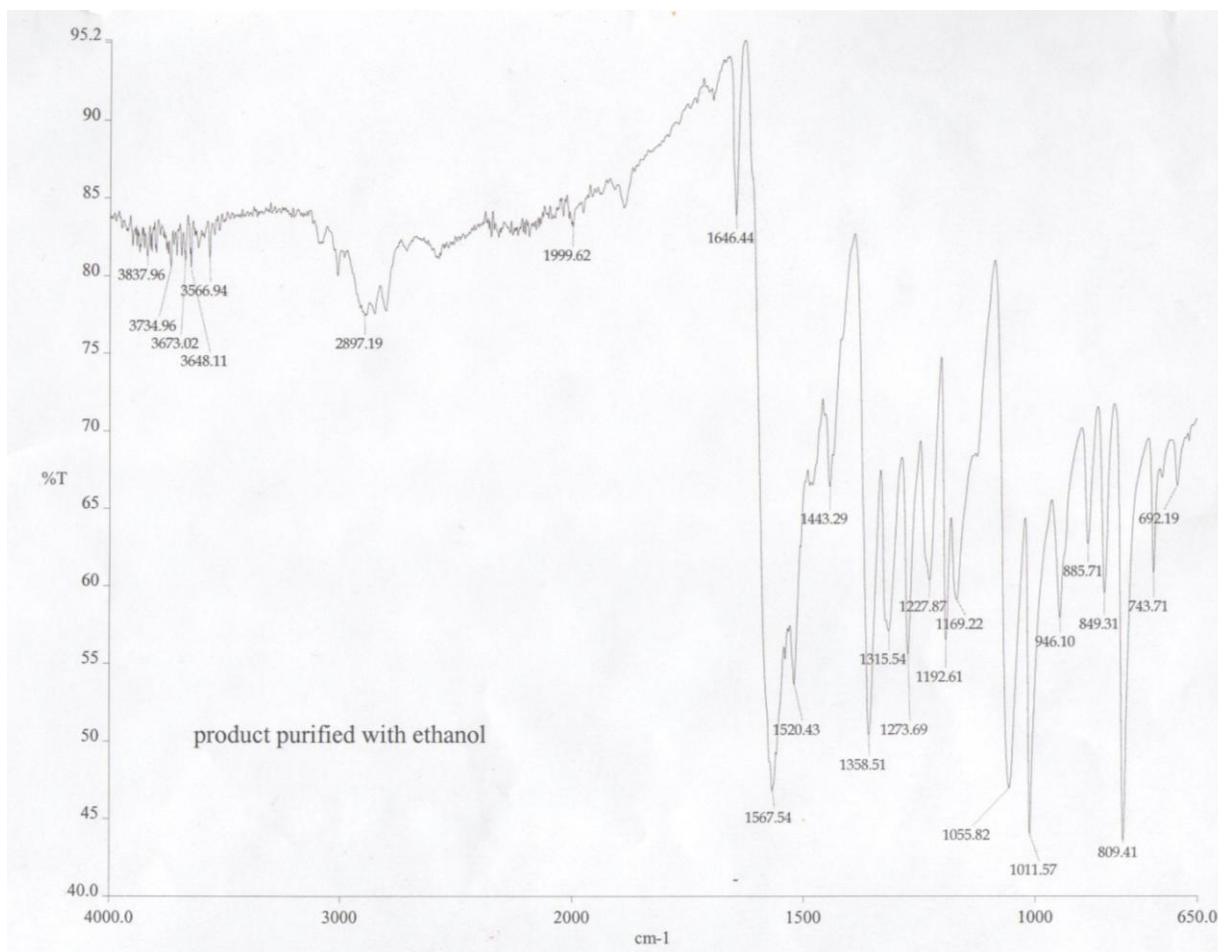


Figure 6: Infrared Spectra of 2dbmac

3. Fluorescence Quantum Yield Determination

The fluorescence quantum yield (Φ_f) is defined as the ratio of the number of photons emitted to the original number of photons absorbed by an analyte, and is calculated mathematically by the equation

$$\Phi_c = \Phi_s \frac{A_s n_c^2 D_c}{A_c n_s^2 D_s}, \quad (1)$$

where the fluorescence quantum yield, or Φ_s , is obtained from literature for each known standard, A is the absorbance value at a fixed excitation wavelength, n is the refractive index of the solvents employed and D is the computed area under the corrected emission spectrum. The subscripts s and c refer to the standard and compound of interest, respectively. In order to correct the fluorescence emission spectra for instrument response, the literature emission spectrum of N,N-dimethylamino-3-nitrobenzene (N,N-DMANB)² was compared to the experimental emission spectrum of N,N-DMANB measured using the LS-50B status. A set of scale factors were determined every 50 cm⁻¹ between 12,500 and 22,200 cm⁻¹.

Fluorescence quantum yields of **2dbmac** were calculated using a stock solution of fluorescein in 0.1 N NaOH (maximum absorbance of approximately 0.5). The stock solution was accurately diluted tenfold to give an absorbance maximum of approximately 0.05. Optical absorption spectra were generated for both the stock and diluted solutions. A fluorescence emission spectrum of the diluted standard solution was obtained, fixing the excitation wavelength which produced an emission spectrum that started and ended at baseline. The same procedures were followed for each sample in varying solvents of interest. Experimental fluorescence emission data was imported first into Microsoft Excel[®] to convert the data from wavelength to wavenumbers. Then the data was imported into Mathcad[®], which corrected the fluorescence emission spectra of both the standard and the analyte and also computed the

fluorescence quantum yields. Appendix A provides a sample calculation for the fluorescence quantum yield of **2dbmac**.

The same procedures were followed for measuring the fluorescence quantum yields of **2dbmac**, in cyclohexane and n-hexane, with the exception of using coumarin-481 (7-N,N-diethylamino-4-trifluoromethyl-1,2-benzopyrone) in acetonitrile ($\Phi_f = 0.11$) as the standard⁴.

4. Fluorescence Lifetime Determination

The fluorescence lifetime (τ_f) is defined as the inverse of the sum of the first-order radiative and nonradiative rates of decay ($\tau_f = 1/(k_f + k_{nr})$). The fluorescence lifetimes of **2dbmac** were measured using a Photon Technology International® fluorescence lifetime spectrometer equipped with a GL-3300 Nitrogen laser, GL-302 dye laser and GL-303 frequency doubler compartments. In order to prevent quenching of the excited states by oxygen, the solutions were properly degassed by purging with molecular nitrogen gas for approximately five minutes prior to measuring the fluorescence lifetimes. FeliX 32 computer software was used to generate the time-dependent fluorescence decay spectra. The fluorescence decay profile of the instrument response function (IRF) was also generated at the same maximum intensity as that of the sample decay curve. An aqueous non-dairy creamer solution served as the IRF for the fluorescence lifetime measurements. After generating the time-dependent fluorescence decay spectra and the IRF, the data was analyzed using a curve-fitting procedure, measuring both the single and biexponential fluorescence lifetimes. Best-fit curves were chosen based on how well the field fit curve fit the decay sample curve by statistical analysis. Appendix B provides a sample worksheet for fluorescence lifetime determination.

Results and Discussion

1. Introduction

The electronic absorption and fluorescence properties of **2dbmac** were studied in a variety of nonpolar, polar protic, and polar aprotic solvents. The resulting solutions differed in color, ranging from light red to dark red, then peach to orange, and then light yellow to bright yellow as the polarity of the solvents increased. The color change represented the solvent effects on the absorption of light. Fluorescence lifetimes (τ_f) and fluorescence quantum yields (Φ_f) were also calculated in a variety of nonpolar, polar protic, and polar aprotic solvents. Radiative and nonradiative decay constants were calculated as well as solvatochromic and photophysical characteristics and quantum chemical calculations.

2. Electronic Absorption and Fluorescence Properties

The absorption and fluorescence spectra of **2dbmac** in six different solvent, differing in polarity, are shown in Figure 7; the figure demonstrates the solvatochromic properties of the compound. This compound undergoes bathochromic (or red) shifts in going from nonpolar to polar protic and then to polar aprotic solvents. Also, the spectral broadening becomes greater as the solvent polarity increases. Figures 8-10 illustrate the absorption and fluorescence spectra of **2dbmac** in various nonpolar, polar protic and polar aprotic solvents. The figures show that the fluorescence spectra undergo a larger bathochromic (or red) shift than the absorption spectra.

The solvatochromic shifts and spectral broadening are caused by intramolecular charge transfer from the nitrogen atom of the alkylamino group (electron donor) to the carbonyl oxygen atom (electron acceptor). The spectroscopic and photophysical characteristics of **2dbmac** are presented in Table 1. Also listed in the table are the solvent polarity function (Δf) and the empirical scale of solvent polarity ($E_T(30)$) of each solvent. The solvent polarity

function (Δf) is dependent upon both the dielectric constant (ϵ) and the refractive index (n) of the solvent, defined as

$$\Delta f = \frac{\epsilon - 1}{2\epsilon + 1} - \frac{n^2 - 1}{2n^2 - 1} \quad (2)$$

The $E_T(30)$ empirical solvent polarity scale is based on the solvatochromic shift of the first maximum of a betaine dye². Likewise with Δf , the magnitude of $E_T(30)$ is dependent upon solvent polarity.

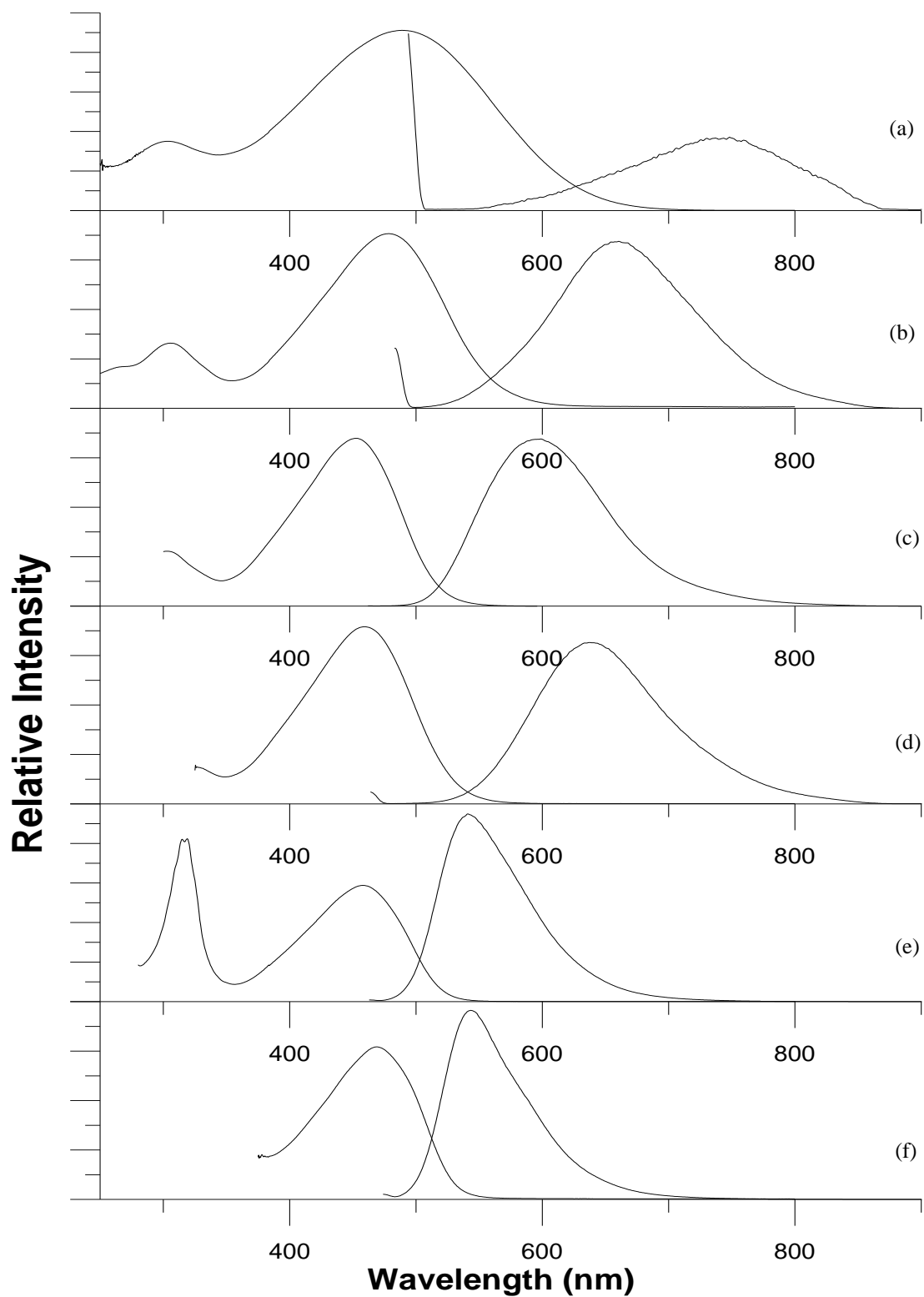


Figure 7: Absorption and fluorescence spectra in (a) 2,2,2-trifluoroethanol; (b) 2-propanol; (c) ethyl acetate; (d) acetone; (e) benzene; (f) carbon disulfide.

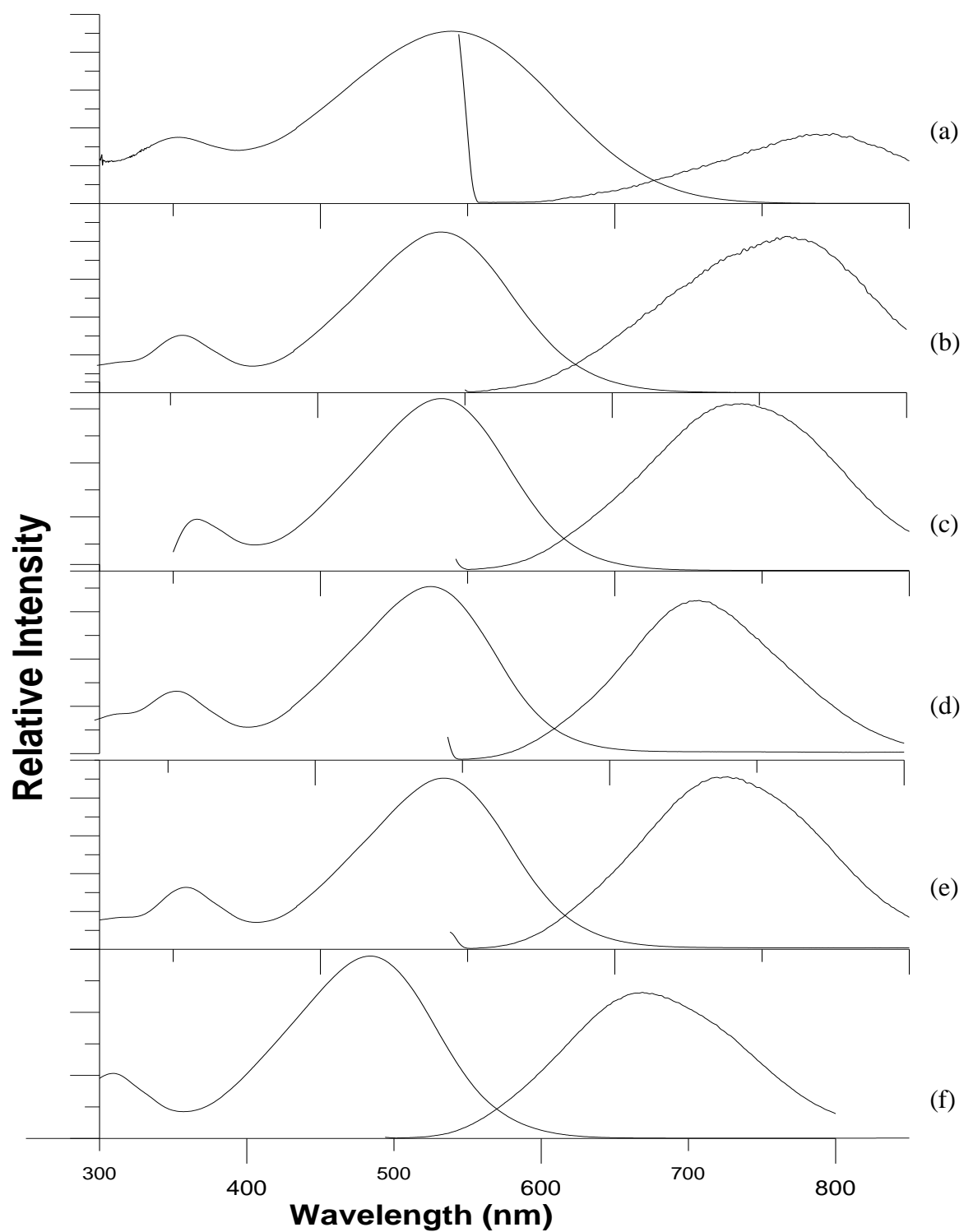


Figure 8: Optical absorption and fluorescence spectra in polar protic solvents, (a) 2,2,2-trifluoroethanol, (b) methanol, (c) ethanol, (d) 2-propanol, (e) 1-propanol, and (f) 1-butanol.

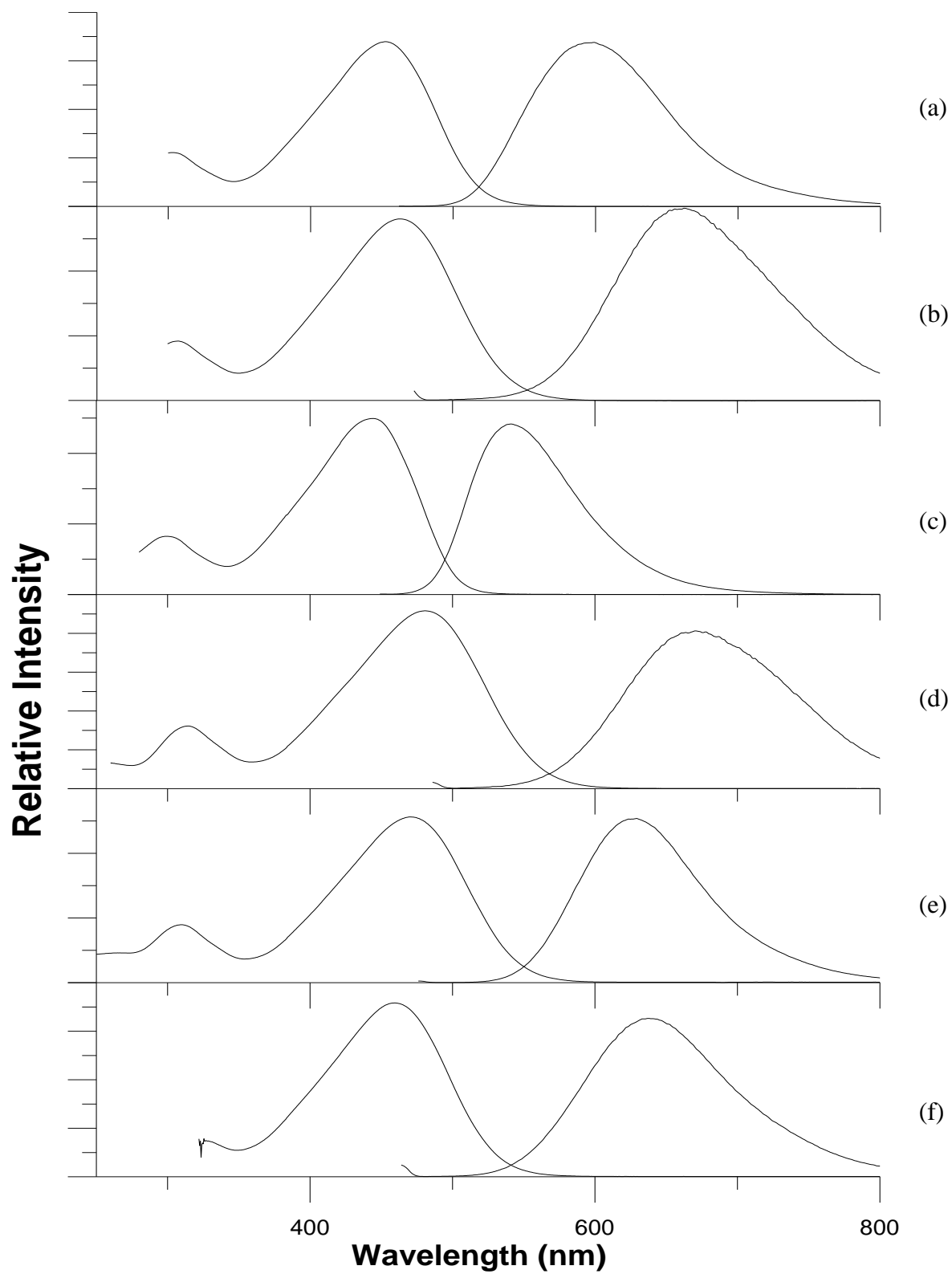


Figure 9: Optical absorption and fluorescence spectra in polar aprotic solvents, (a) ethyl acetate, (b) acetonitrile, (c) diethyl ether (d) dimethyl sulfoxide, (e) dichloromethane, and (f) acetone.

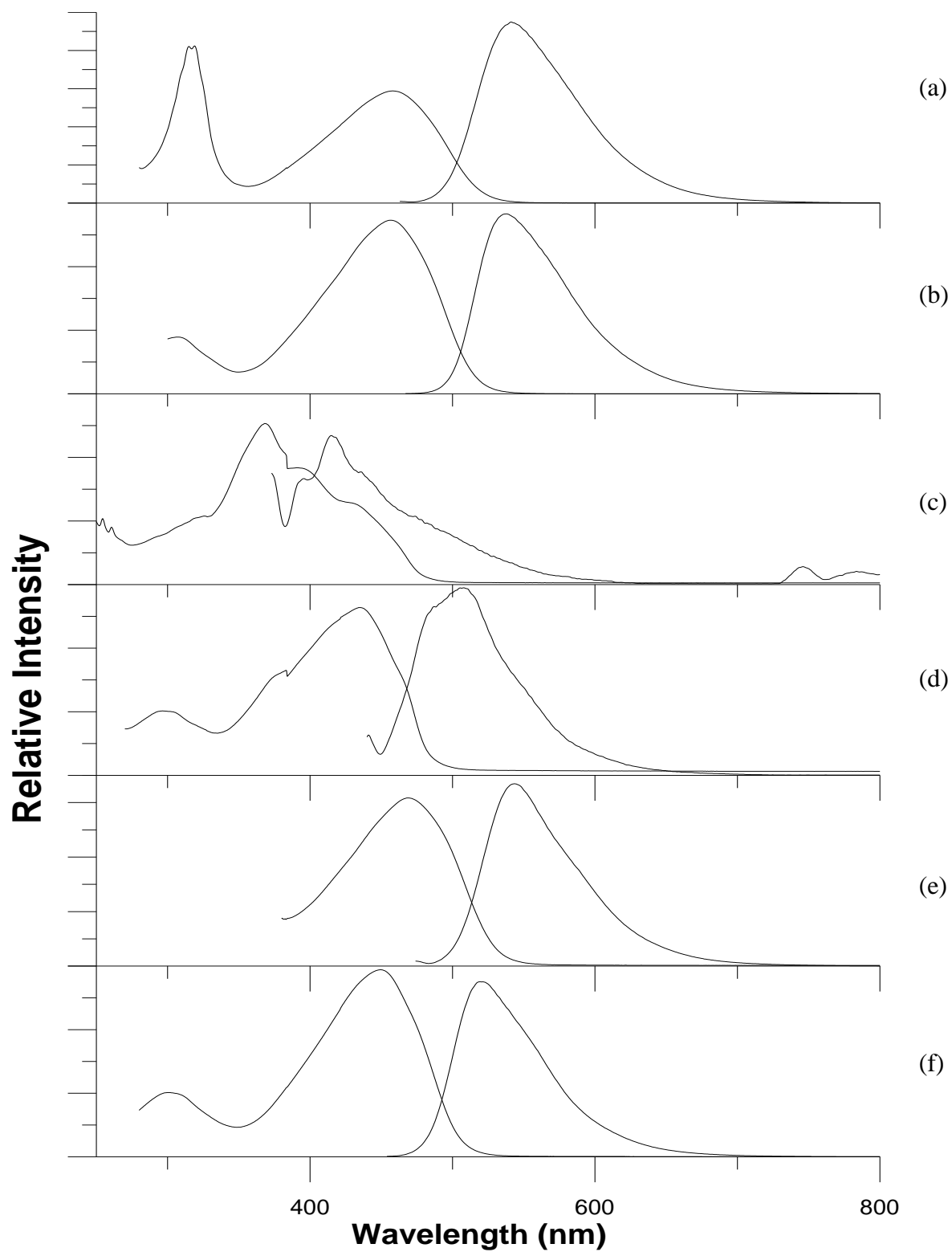


Figure 10: Optical absorption and fluorescence spectra in nonpolar solvents, (a) benzene, (b) toluene, (c) n-hexane, (d) cyclohexane, (e) carbon disulfide, and (f) carbon tetrachloride.

Table 1: Spectroscopic and photophysical characteristics of 2dbmac in various solvents

Solvent	ν_{abs} (cm^{-1})	ν_{flu} (cm^{-1})	Δf^*	$E_T(30)^*$ (kcal mol^{-1})	ϕ_f	τ_f (s)	k_f (s^{-1})	k_{nr} (s^{-1})
EtOH	20762.8 (481.63nm)	14577.0 (686.01nm)	0.2887	51.9	0.035	5.1E-10	68992706	1902227479
MeOH	20685.9 (483.42nm)	13912.5 (718.78nm)	0.3093	55.4	9.246*10 ⁻³	2.8E-10	33021429	3538407143
1-PrOH	20646.7 (484.34nm)	14782.8 (676.46nm)	0.2746	50.7	0.067	5.2E-10	128450920	1788726994
2-PrOH	20899.1 (478.49nm)	15137.3 (660.62nm)	0.2769	48.4	0.109	3.6E-10	303114572	2477753059
1-BuOH	20661.2 (484.00nm)	14953.5 (668.74nm)	0.2642	50.2	0.072	3.7E-10	196345787	2530679029
TFE	20449.1 (489.02nm)	13364.2 (748.27nm)	0.3159	59.4	6.399*10 ⁻³	2.4E-10	26662500	4140004167
ACN	21590.8 (463.16nm)	15086.4 (662.85nm)	0.3054	45.6	0.041	2.9E-10	140941904	3296665521
DCM	21250.4 (470.58nm)	15895.7 (629.10nm)	0.2171	40.7	0.271	1E-09	261078998	702312139
DMSO	20800.8 (480.75nm)	14907.6 (670.80nm)	0.2637	45.1	0.041	3.2E-10	129870130	3037694013
EtOAc	22109.2 (452.30nm)	16694.8 (598.99nm)	0.1996	38.1	0.183	6.2E-10	295018539	1317104627
Acetone	21764.2 (459.47nm)	15697.8 (637.03nm)	0.2843	42.2	0.087	4.2E-10	207538168	2177958015
Diethyl Ether	22546.9 (443.52nm)	18474.4 (541.29nm)	0.1669	34.5	0.060	5.7E-10	104712042	1640488656
Toluene	21904.8 (456.52nm)	18588.7 (537.96nm)	0.0131	33.9	0.186	4.2E-10	439197166	1922077922
n-hexane	27165.1 (368.12nm)	24101.6 (414.91nm)	-0.0004	31.0	3.436*10 ⁻³	1.1E-09	3123636	905967273
Cyclohexane	22966.9 (435.41nm)	19690.1 (507.87nm)	-0.0004	30.9	5.809*10 ⁻³	4.9E-10	11855102	2028961224
Benzene	21834.5 (457.99nm)	18483.9 (541.01nm)	0.0031	34.3	0.222	5.6E-10	398492192	1396517681
CS ₂	21313.3 (469.19nm)	18398.6 (543.52nm)	-0.0007	32.8	0.267	6.6E-10	404913558	1111616621
CCl ₄	22248.9 (449.46nm)	19223.7 (520.19nm)	0.0119	32.4	0.125	5.2E-10	239142912	1674000383

*² Both Δf and $E_T(30)$ values are taken from Suppan, P. and Ghonheim, N., in *Solvatochromism*, The Royal Society of Chemistry, Cambridge, 1997.

Absorption and fluorescence properties of **2dbmac** were plotted against both Δf and the $E_T(30)$ empirical solvent polarity scale; these graphs are shown in Figures 11 and 12.

Solvatochromic properties are observed, for both Δf and $E_T(30)$, depicting decreasing absorption and fluorescent wavenumbers with respect to an increase in solvent polarity. The observed graphical solvatochromic properties are consistent with a charge transfer electronic transition.

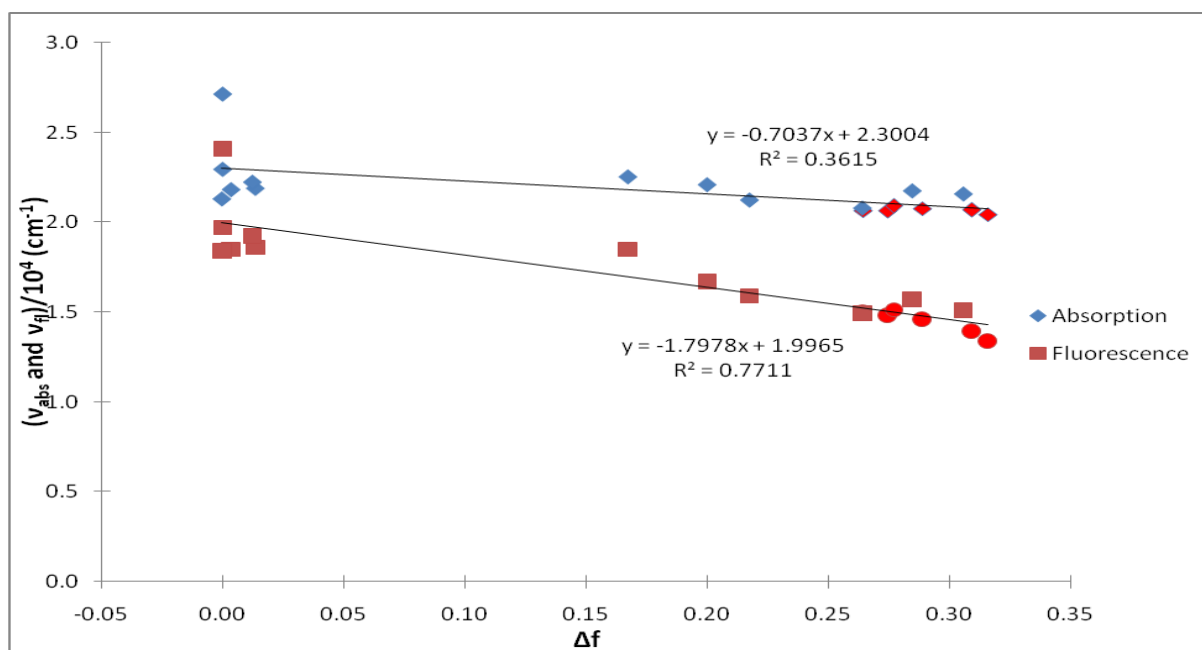


Figure 11: Plot of maximum absorption and fluorescent wave numbers of 2dbmac against Δf in various polar protic, polar aprotic and nonpolar solvents. The alcohols are designated by the red shaped diamonds and circles.

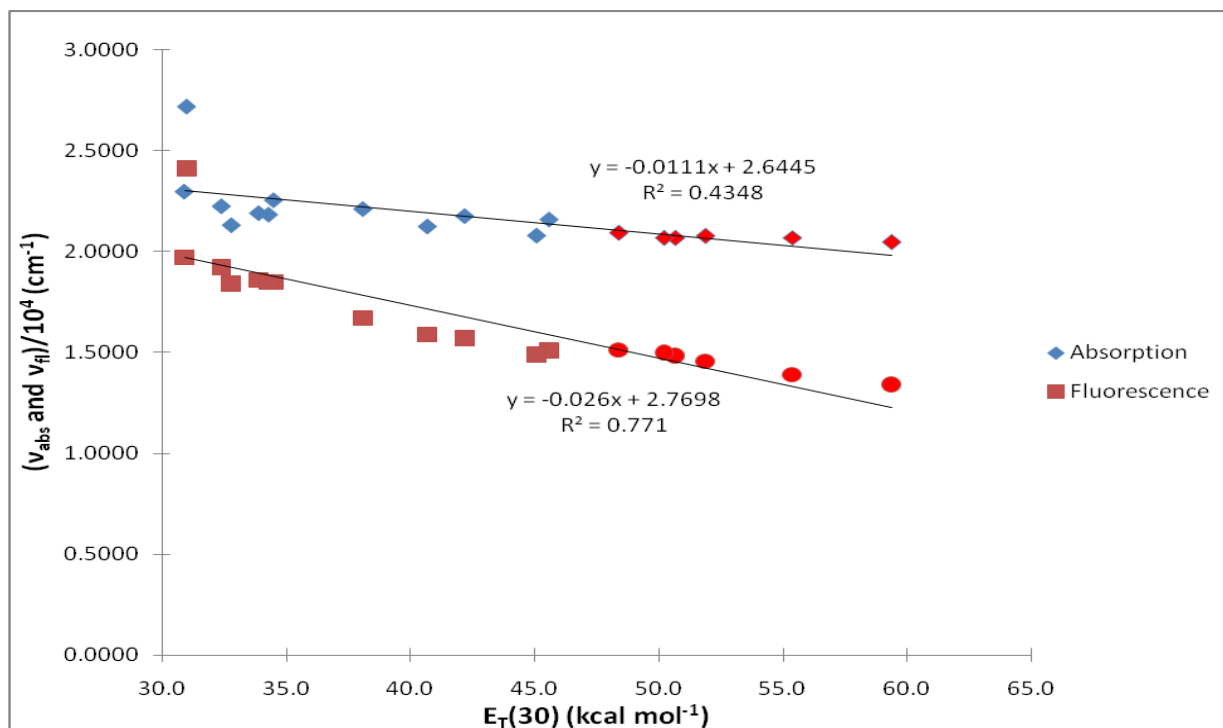


Figure 12: Plot of maximum absorption and fluorescent wave numbers of 2dbmac against $E_T(30)$ in various polar protic, polar aprotic and nonpolar solvents. The alcohols are designated by the red shaped diamonds and circles.

Experimental Data from the fluorescence lifetimes (τ_f) and fluorescence quantum yields (Φ_f) show a solvent dependence for the compound. Both Φ_f and τ_f parameters are used to calculate the first-order radiative and nonradiative decay constants of the first-excited singlet state of **2dbmac**. The first-order radiative decay constant, k_f , can be calculated from the equation:

$$k_f = \frac{\Phi_f}{\tau_f}, \quad (3)$$

where Φ_f is the fluorescence quantum yield and τ_f is the fluorescence lifetime. Also, the first-order nonradiative decay constant, k_{nr} , can be calculated from the equation:

$$k_{nr} = \left(\frac{1}{\Phi_f} - 1 \right) k_f. \quad (4)$$

Both the first-order radiative and nonradiative decay constants are plotted against the maximum fluorescent wavenumbers, of **2dbmac**, in a variety of nonpolar, polar protic, and polar aprotic solvents, as illustrated in Figure 13. Graphical observations show that solvent has little influence on the radiative rate of decay, but more significant influence on the nonradiative rate of decay. Between 22,000 and 15,500 cm^{-1} (nonpolar to moderately polar solvents), there is a slight decrease in k_{nr} . Below 15,500 cm^{-1} (polar protic to aprotic solvents), a significant increase in k_{nr} is observed.

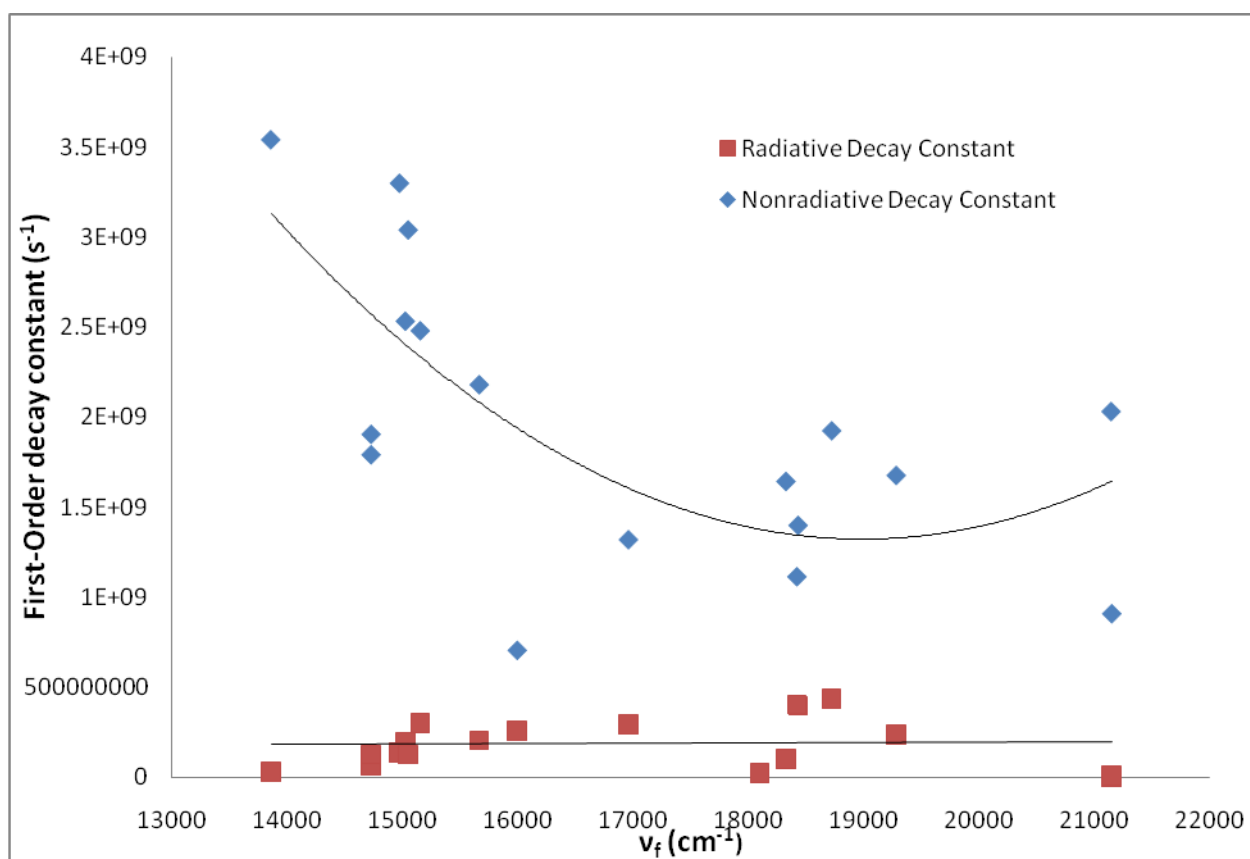


Figure 13: Plot of first-order decay constants as a function of fluorescent wavenumbers of **2dbmac** in various aprotic and protic solvents.

The behavior of k_{nr} can be explained by the energy gap law, which predicts an exponential dependence of k_{ic} on ΔE , the energy gap between S_0 and S_1 , respectively⁵:

$$k_{ic} = Ce^{-\alpha\Delta E}, \quad (5)$$

where C and α are constants.

In accordance with the energy gap law of internal conversion for excited states, the first-order nonradiative decay constant, k_{nr} , is predicted to increase as the energy gap between S_0 and S_1 decreases due to greater vibrational overlap between the S_0 and S_1 states. In Figure 13, k_{nr} decreases for the set of data of **2dbmac** from 21160 cm^{-1} (n-hexane) to 15671 cm^{-1} (acetone). The decreased trend demonstrates anti-energy gap behavior in this region. The deviation from the energy gap law in less polar solvents may be related to the location of the (n, π^*) state and its influence on intersystem crossing.

In the next section, quantum chemical calculations show that for **2dbmac**, the $S_0 \rightarrow S_1$ transition is (CT, π, π^*) and the $S_0 \rightarrow S_2$ transition is predicted to be (n, π^*) for the compound. A similar order is expected for the triplet states. Figure 14 illustrates a Jablonski state energy-level diagram of the various types of radiative and nonradiative transitions that occur in electronic systems and the effect of solvent polarity on the energy levels.

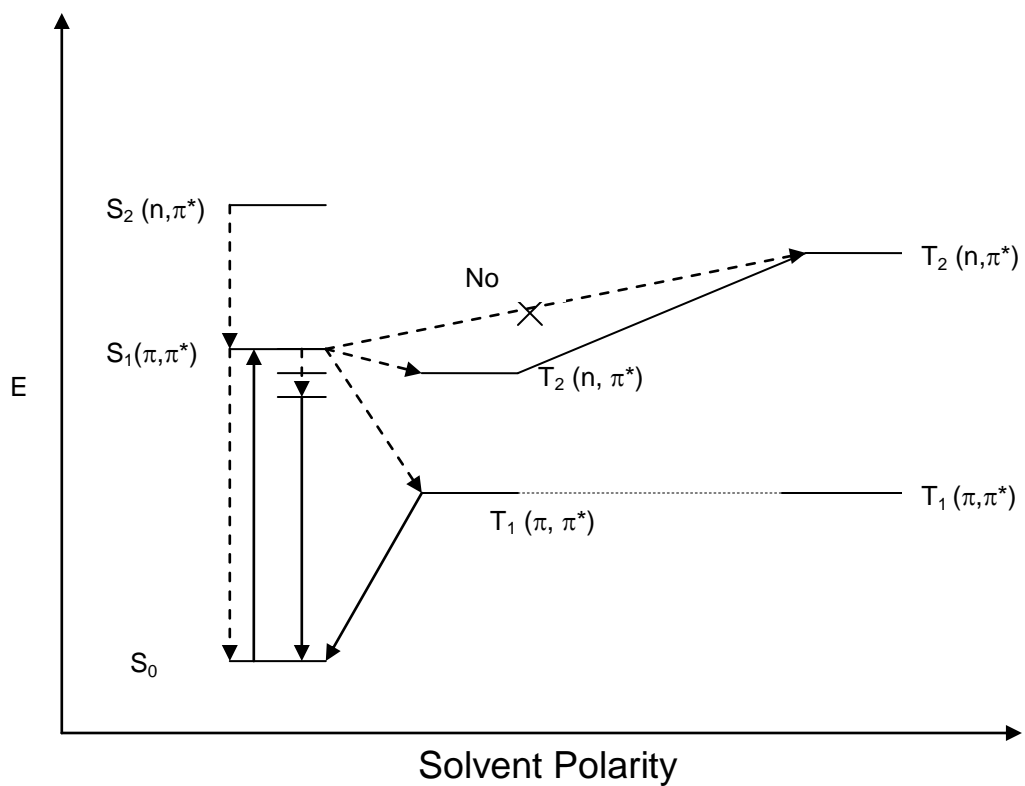


Figure 14: Jablonski diagram of the effect of solvent on (π, π^*) and (n, π^*) states. Solid lines represent radiative transitions and dashed lines represent nonradiative transitions.

The fluorescence quantum yields of **2dbmac** were also plotted against the maximum fluorescent wavenumbers (ν_{fl}) in a variety of nonpolar, polar protic and polar aprotic solvents, shown in Figure 16.

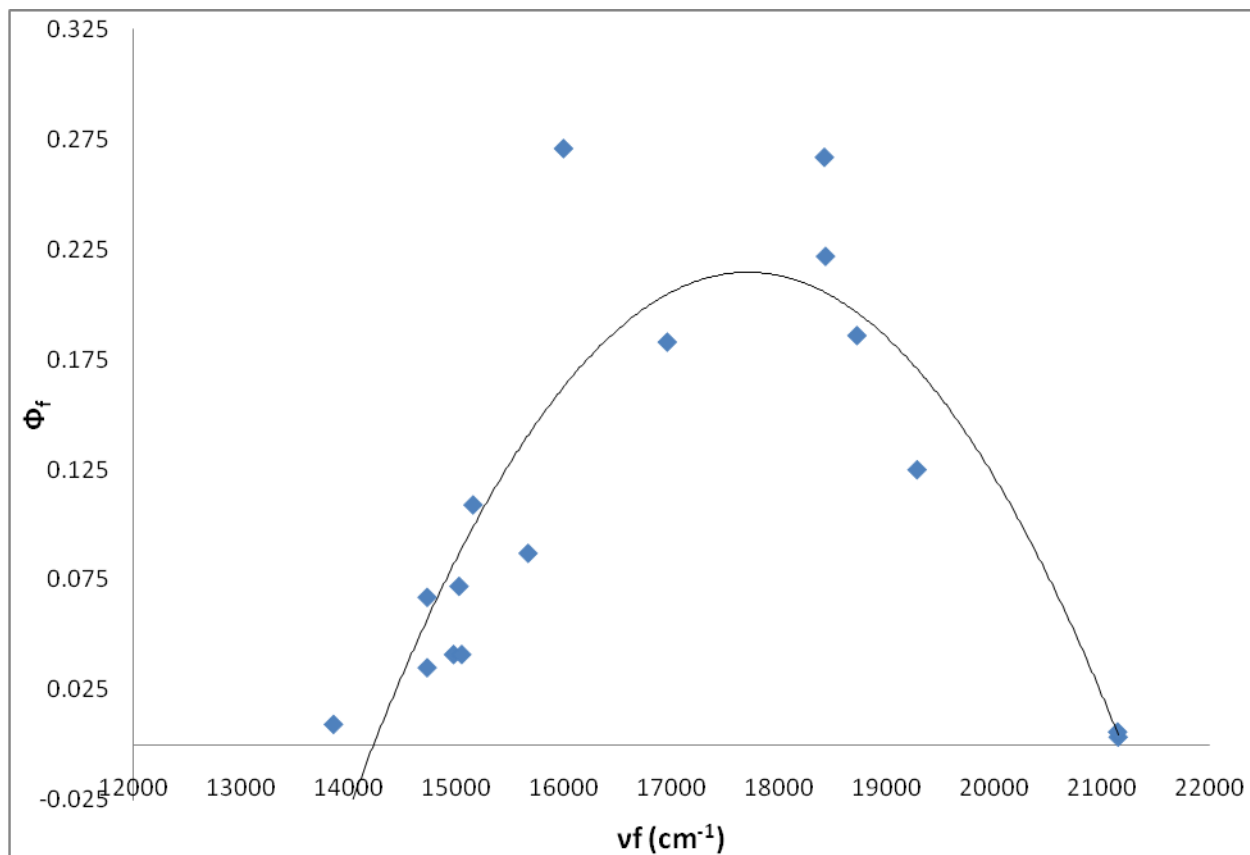


Figure 15: Plot of the fluorescence quantum yield of **2dbmac** against ν_{fl} in various protic and aprotic solvents

The quantum yields reach a maximum for solvents of moderate polarity, as observed in the figure above, which is consistent with the trend in k_{nr} . Rearrangement and algebraic substitution of equations (3) and (4), along with $\tau_f = 1/(k_f + k_{nr})$, results in the fluorescence quantum yield (Φ_f) of an electronic system equation expressed below as

$$\Phi_f = \frac{k_f}{k_f + k_{nr}}, \quad (6)$$

where $k_{nr} = k_{ic} + k_{isc}$. Equation (6) can be used to explain the trends observed in Figures 15. As k_{nr} decreases, Φ_f increases until a maximum is reached in Φ_f and a minimum is reached with k_{nr} . At the peak point, k_{nr} starts to increase and Φ_f decreases.

Lippert-Mataga plots were also constructed for **2dbmac** from the spectroscopic data, shown in Figure 17. Lippert-Mataga plots directly relate the Stoke's shift for a molecule in different solvents to the solvent polarity function. The Stoke's shift, $\Delta\nu$, is the energy difference, in wavenumbers, between the absorption and fluorescence spectral maxima, related linearly to Δf by the Lippert-Mataga equation⁶:

$$\Delta\nu = \frac{2\Delta\mu^2}{hca^3} \Delta f + \Delta\nu_0, \quad (7)$$

where $\Delta\mu = \mu_e - \mu_g$ is the difference between the excited-state and the ground-state dipole moments, h is Planck's constant (6.626×10^{-34} J s), c is the speed of light in a vacuum (2.998×10^8 m s⁻¹) and a is the Onsager cavity radius for the spherical interaction of the dipole in a solvent, respectively. Thus, a plot of $\Delta\nu$ as a function of Δf yields a straight line slope equal to $2\Delta\mu^2/hca^3$. The resulting equation can be used to calculate the excited state dipole moment of the chemical species since both a and μ_g are determined computationally. Computed results yielded an Onsager cavity radius equal to 5.98 Å and a ground state dipole moment equal to 4.80D. Using the Lippert-Mataga method, the excited state dipole moment for **2dbmac** was calculated to be 15.24D. The large increase in dipole moment is consistent with charge transfer. The quantum chemical calculations in the next section support the charge transfer theory.

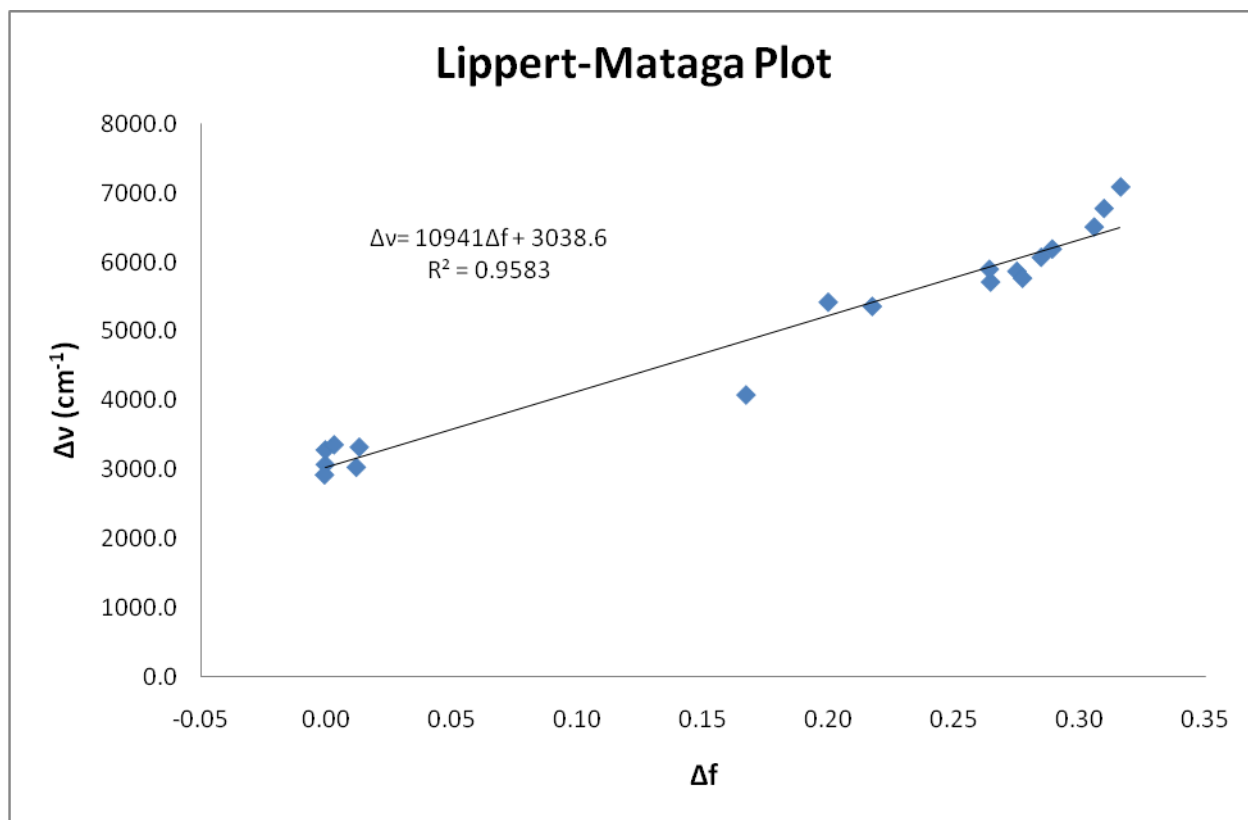


Figure 16: Lippert-Mataga Plot of Stoke's shift ($\Delta\nu$) against Δf of **2dbmac** in various polar protic, polar aprotic and nonpolar solvents.

3. Quantum Chemical Calculations

DFT B3LYP/6-31G(d) geometry optimization and TD-DFT spectral calculations were performed on **2dbmac**. The computed molecular orbitals of the compound are illustrated in Figure 18. Calculations show that the $S_0 \rightarrow S_1$ electronic transition for **2dbmac** occurs via an intramolecular charge transfer (CT, π , π^*) mechanism. The electron density is distributed along the cross-conjugated π system in the computed HOMO, with significant density on the tertiary nitrogen atom of the alkylamino group. In the LUMO, electron density is transferred from the nitrogen atoms to the carbonyl center, signifying a charge transfer process. In addition, the $S_0 \rightarrow S_2$ electronic transition is predicted to be (n , π^*). Table 2 lists the molecular orbital

calculations of **2dbmac** as well as the corresponding oscillator strengths (f) of each transition, which measures the strength of the electronic transition.

Table 2: Computed Molecular Orbital Calculations of **2dbmac**

HOMO-->LUMO	(CT, π , π^*)
$\lambda=470.82\text{nm}$	$f=1.9725$
HOMO-2-->LUMO	(n, π^*)
$\lambda=429.93\text{nm}$	$f=0.000$

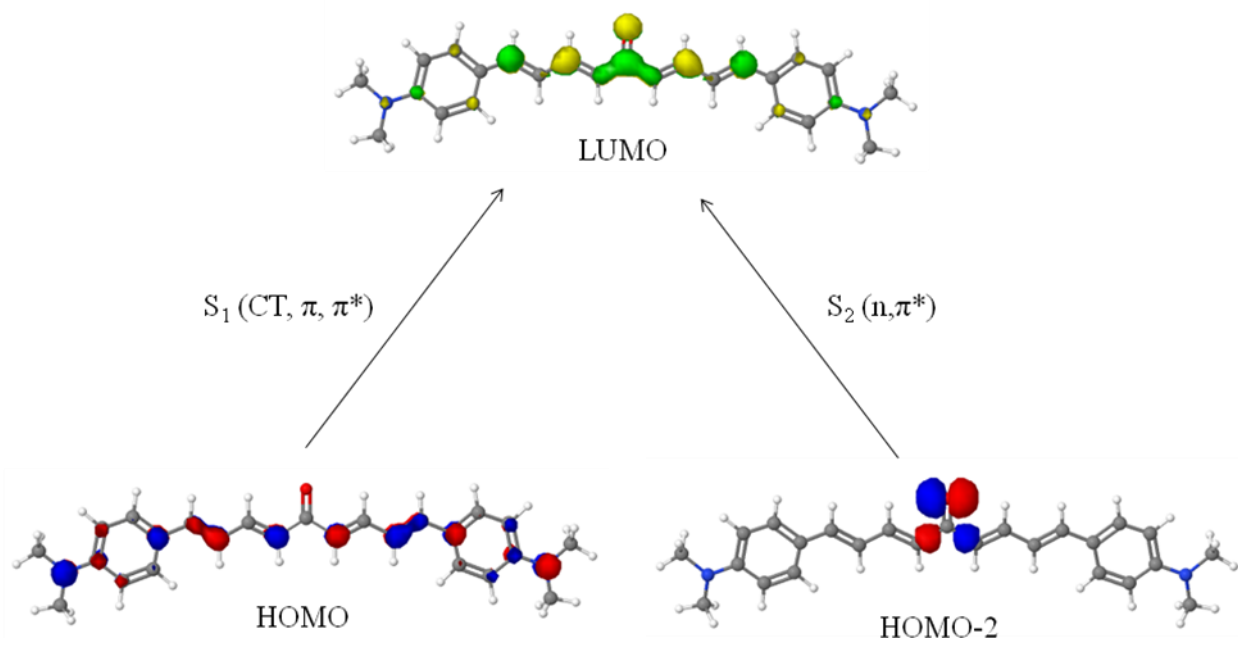


Figure 17: Computed molecular orbitals of **2dbmac**.

The dipole moments, the atomic charges of the tertiary nitrogen and the carbonyl oxygen, and the absorbance maximums were also compared, listed in Tables 3 and 4. The percent difference of less than 15% shows good precision and accuracy. The ground-state dipoles show an increasing trend as the polarity of the solvent increased. The atomic charge of the tertiary nitrogen decreases with increasing solvent polarity and the atomic charge of the carbonyl oxygen increases with increasing solvent polarity; these trends are illustrated in Tables 3 and 4.

Table 3: Dipole and Atomic Charges for the trans/trans structure of **2dbmac**

solvent	μ (D)	3° N	Carbonyl O
Gas (without solvent)	4.8029	-0.472	-0.5214
Cyclohexane	5.4132	-0.4709	-0.5476
Acetonitrile	6.5279	-0.4687	-0.5881
Water	6.6139	-0.4687	-0.5909

Table 4: Theoretical and Experimental Absorbance Maximums

solvent	Theoretical λ max	Experimental λ max	Percent Error
Cyclohexane	503.69 nm	435.41nm	13.56
Acetonitrile	527.65nm	463.16nm	12.22
Water	528.86nm	N/A	N/A

Note: The experimental absorbance maximum could not be taken in deionized water because **2dbmac** is not soluble in water.

Conclusions

Experimental results demonstrate that 2dbmac exhibits solvatochromic properties in various protic and aprotic solvent systems. The spectroscopic characteristics show linear relationships when plotted against both Δf and the $E_T(30)$ scale, which is consistent with electronic charge transfer. The fluorescence lifetime and quantum yields vary depending on the solvent's nature. The changes in the nonradiative rate of decay contribute to the variations in the photophysical parameters. The relationship between ν_{fl} and k_{nr} in polar solvents is consistent with the energy gap law for internal conversion and in nonpolar to moderately polar solvents, the deviation with the energy gap law may be associated with the location of the (n, π^*) state and its influence on the intersystem crossing. Lastly, the quantum chemical calculations indicate that the S_1 state occurs by an intramolecular charge transfer (π, π^*) mechanism and S_2 is predicted to be (n, π^*) for the compound.

References

- [1] Connors, R. E.; Ucak-Astarlioglu, M. G. *J. Phys. Chem. A* **2003**, *107*, 7684.
- [2] Suppan, P.; Ghonheim, N. *Solvatochromism*; Royal Society of Chemistry: Cambridge, 1997.
- [3] Lakowicz, J. R. *Principles of Fluorescence Spectroscopy*, 2nd ed.; Springer: New York, 2004.
- [4] Rechthaler, K.; Kohler, G.; *Chem. Phys. Lett.* **1994**, *189*, 99.
- [5] Klessinger, M.; Michl, J. *Excited States and Photochemistry of Organic Molecules*; VCH Publishers: New York, 1995.
- [6] Nad, S.; Pal, H. *J. Phys. Chem. A* **2001**, *105*, 1097.

Appendix A: Fluorescence Quantum Yield Sample Calculation

Connors

Quantum yield determination for 2dbmac in undegassed Toluene
with red sensitive tube.
experiment 1

This QuickSheet demonstrates Mathcad's **cspline** and **interp** functions for connecting X-Y data.



Enter a matrix of X-Y data to be interpolated:

Enter spectral data for **compound** after converting to wavenumbers, multiplying intensity by lambda squared **DO NOT** normalize intensity. Insert data from Excel -right key, paste table.

data1 :=

1052.63	$3.08 \cdot 10^6$
1030.49	$3.05 \cdot 10^6$
21008.4	$3.01 \cdot 10^6$
0986.36	...

Click on the **Input Table** above until you see the handles, and enlarge it to see the matrix **data** used in this example.

data1 := csort(**data1**, 0)

X := **data1** <0>

Y := **data1** <1>

Spline coefficients:

S1 := cspline(X, Y)

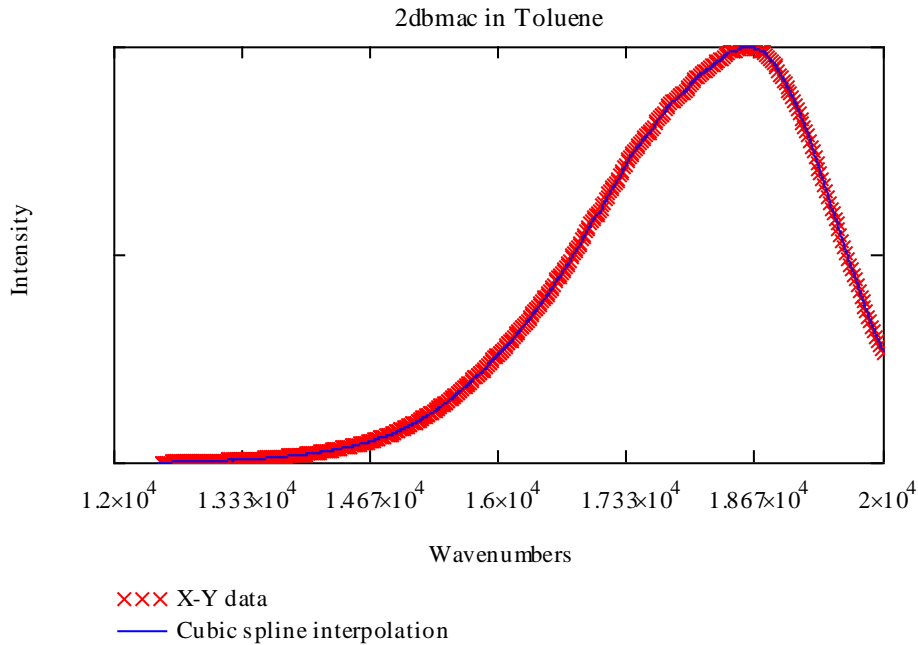
Fitting function:

fit(x) := interp(S1, X, Y, x)

Sample interpolated values:

$$\text{fit}(21000) = 2.994 \times 10^6$$

$$\text{fit}(18800) = 1.099 \times 10^7$$



Correction factors for LS50B with red sensitive tube

DATA Limits 12,500-22,200 Wavenumbers

corrdata :=

	0	1
0	12500	4.43
1	12550	...

xdata := csort (corrdata ,0)

A := corrdata <0> B := corrdata <1>

Spline coefficients:

S := cspline(A, B)

Fitting function:

Fitting function:

corrfit(x) := interp(S, A, B, x)

corrspec(x) := corrfit(x)·fit(x)

$\lambda := 12500 \dots 22200$

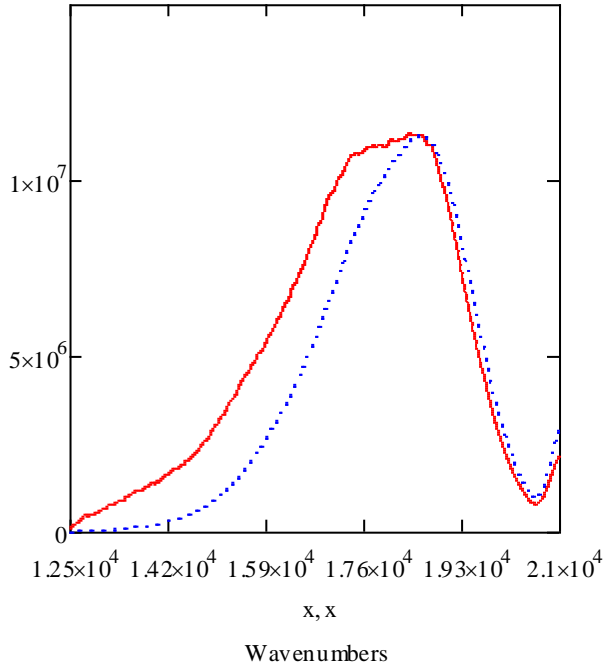
l =

$1.25 \cdot 10^4$
$1.255 \cdot 10^4$
$1.26 \cdot 10^4$
...

corrspec(l) =

$9.097 \cdot 10^4$
$2.096 \cdot 10^5$
$2.853 \cdot 10^5$
$3.312 \cdot 10^5$
...

corrspec(x)
fit(x)



$$\int_{12500}^{20550} \text{fit}(x) \, dx = 3.431 \times 10^{10}$$

$$\int_{12500}^{20550} \text{corrspec}(x) \, dx = 4.351 \times 10^{10}$$

Enter a matrix of X-Y data to be interpolated:

Enter spectral data for **standard** (fluorescein) after converting to wavenumbers, multiplying intensity by lambda squared DO NOT normalize intensities. Insert data from Excel -right key, paste table.

stdata :=

21052.63	$3.73 \cdot 10^6$
21030.49	$3.74 \cdot 10^6$
21008.4	...

Click on the **Input Table** above until you see the handles, and enlarge it to see the matrix **data** used in this example.

```
stdata := csort (stdata , 0)
```

```
C := stdata <0>      D := stdata <1>
```

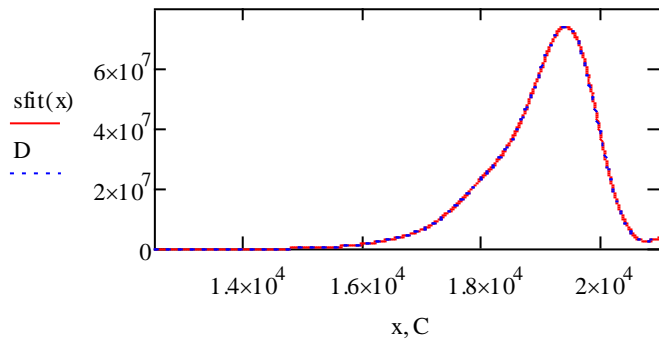
Spline coefficients:

```
S := cspline(C,D)
```

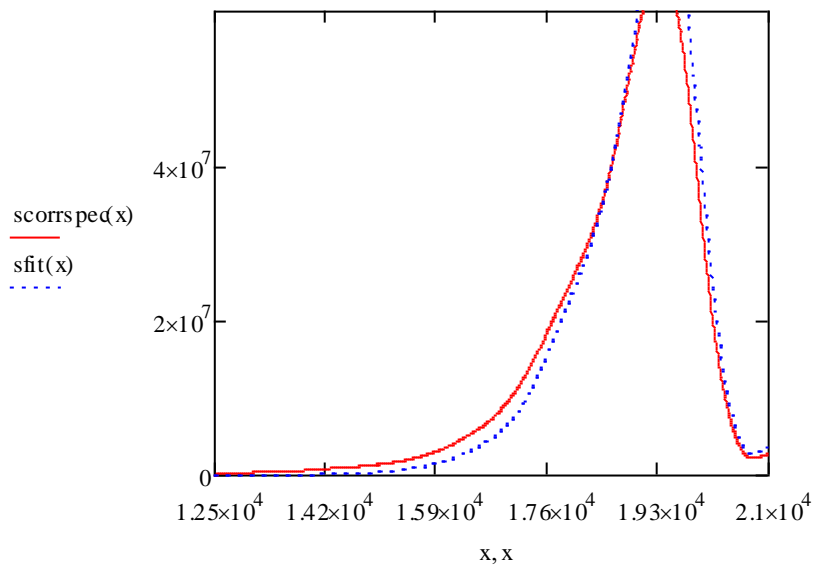
Fitting function:

```
sfit(x) := interp(S,C,D,x)
```

$$\text{sfit}(18000) = 2.401 \times 10^7$$



```
scorspec(x) := corfit(x)·(sfit(x))
```



Compound

$$\int_{12500}^{20550} \text{corrspec}(x) dx = 4.351 \times 10^{10}$$

Standard

$$\int_{12500}^{20550} \text{scorrsec}(x) dx = 1.299 \times 10^{11}$$

Area under corrected compound curve

$$D_c := \int_{12500}^{20550} \text{corrsec}(x) dx$$

$$D_c = 4.351 \times 10^{10}$$

Area under corrected standard curve

$$D_s := \int_{12500}^{20550} \text{scorrsec}(x) dx$$

$$D_s = 1.299 \times 10^{11}$$

Compound

$$A_c := 0.0442$$

Toluene

$$n_c := 1.496$$

Standard

$$A_s := 0.0231$$

NaOH

$$n_s := 1.41$$

Absorbance at (ex)
Index of refraction

quantum yield of
standard

$$QY_s := 0.9$$

$$QY_c := QY_s \left(\frac{A_s}{A_c} \right) \cdot \left(n_c \cdot \frac{n_c}{n_s \cdot n_s} \right) \cdot \left(\frac{D_c}{D_s} \right)$$

$$QY_c = 0.186$$

Appendix B: Fluorescence Lifetime Sample Calculation

Fluorescence Lifetime Determination of 2dbmac in Acetonitrile

Single Exponential Lifetime Data

Analysis Function : Tue Dec 09 2008 at 12:48

***** one-to-four exponentials *****

***** Input Values *****

Decay curve : A1 463.16:662.85
IRF curve : A1 463.16:463.16

Start Time : 41
End Time : 50

Offset fixed at -18.5
Shift fixed at 0.46

Pre-exp. 1 : 1
Lifetime 1 : 1

***** Statistics *****

Job done after 6 iterations in 0.047 sec.

Fitted curve : FLD Fit (1)
Residuals : FLD Residuals (1)
Autocorrelation : FLD Autocorrelation (1)
Deconvolved Fit : FLD Deconvoluted (1)

Chi2 : 1.123
Durbin Watson : 2.041
Z : -0.0241

Pre-exp. 1 : 3.693 ± 1.161e-001 (100 ± 3.144%)
Lifetime 1 : 0.2909 ± 9.363e-003

F1 : 1

Tau-av1 : 0.2909
Tau-av2 : 0.2909

Offset : -18.5
Shift : 0.46

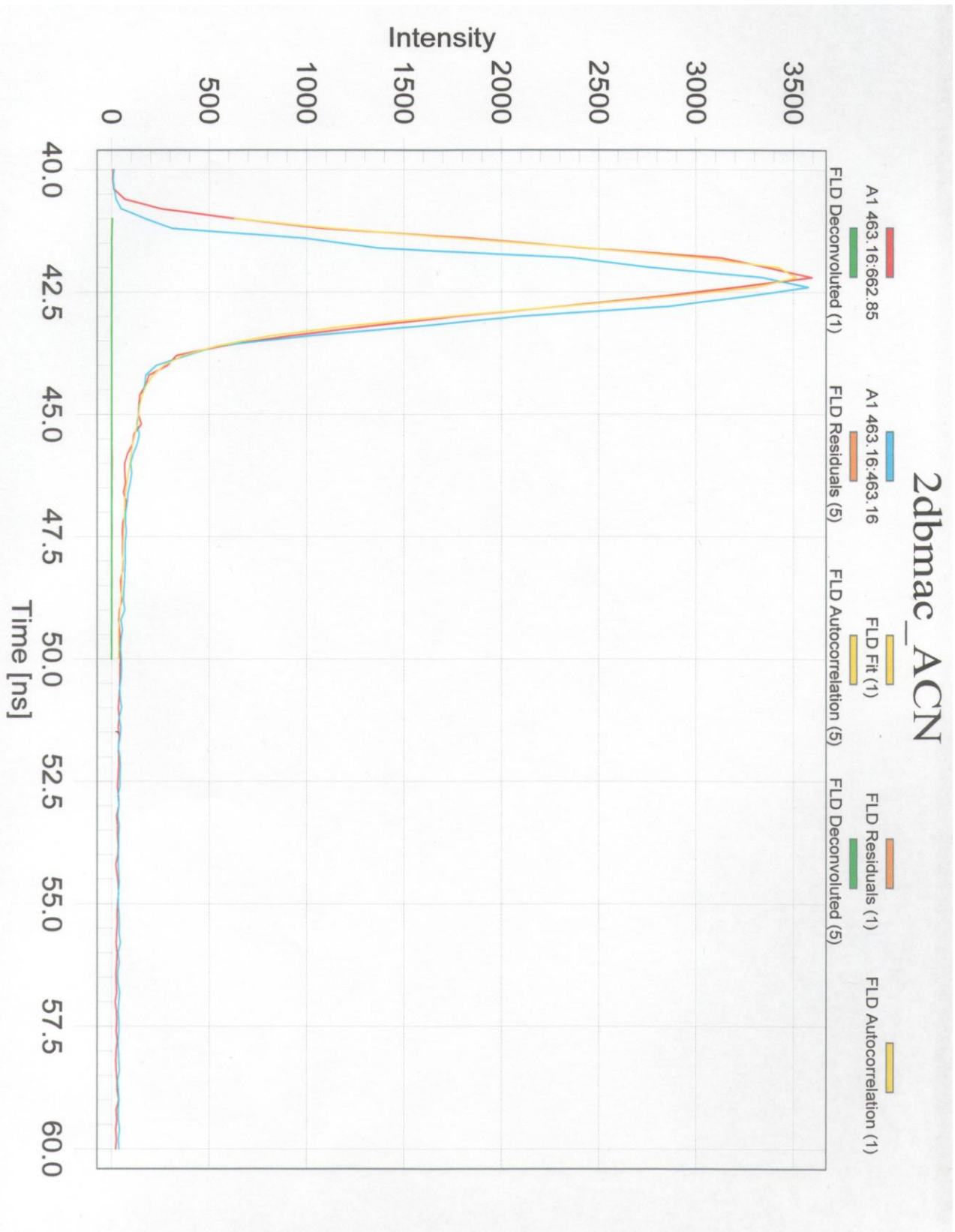


Figure 18: Fluorescence Lifetime of 2dbmac in Acetonitrile